Joint Report of PalMod Projects 989, 1030, and 1192

Project: 989

Project title: PalMod WG1, Physical System

Project lead: Gerrit Lohmann (AWI), Gregor Knorr (AWI), Volker Klemann (GFZ), Uwe Mikolajewicz (MPI)

Report period: 2025-01-01 to 2025-12-31

Overview

During the allocation period of 2025 the project was impacted by a severe cut by the WLA. To continue modelling work during critical production towards the end of PalModIII, a significant portion of simulations were carried out with DKRZ resources from outside project ba0989. This involved AWI and MPI shares at DKRZ. General lack of resources has also been reflected by the fact that project ba0989 has not lost a single node hour as a result of end-of-the-quarter cuts. We are grateful to the WLA that additional resources were granted after QII. Still, a substantial number of simulations had to be postponed to the next allocation period (see proposal 2026).

Report

Work at AWI

WP1.3 continued transient glacial inception until 70 ka (Fig. 1) and aims to prolong the simulation until 50 ka BP using an acceleration of 20. We find continuous growth of ice sheets across Northamerica that starts at about 115 ka BP temperature-controlled in proximity to Baffin Island and Quebec in absence of any significant precipitation change. Thereafter, increased precipitation at the southern border of the evolving Laurentide ice sheet favors further growth, potentially via similar feedback as described by Lu et al. (2024) (WP1.2). Variability of ice volume change follows summer insolation at 65°N, and thereby precession. While growth variability is in agreement with global mean sea level reconstructed by Pico et al. (2017) and Spratt and Lisiecki (2016), we observe dampening and absence of phases of ice volume reduction. Comparison of simulated ice sheet height and extent is in good agreement with the reconstruction by Gowan et al. (2021), except for the Cordilleran ice sheet, that is simulated too large, and absence of the reconstructed Hudson Bay ice shelf. Proposed continuation of the simulation will show whether growth continues beyond 70 ka BP. Redoing part of the simulation with smaller acceleration and additional bias-correction of seawater temperature will illustrate relevance of ice-ocean feedbacks for the simulated variability of the ice sheet.

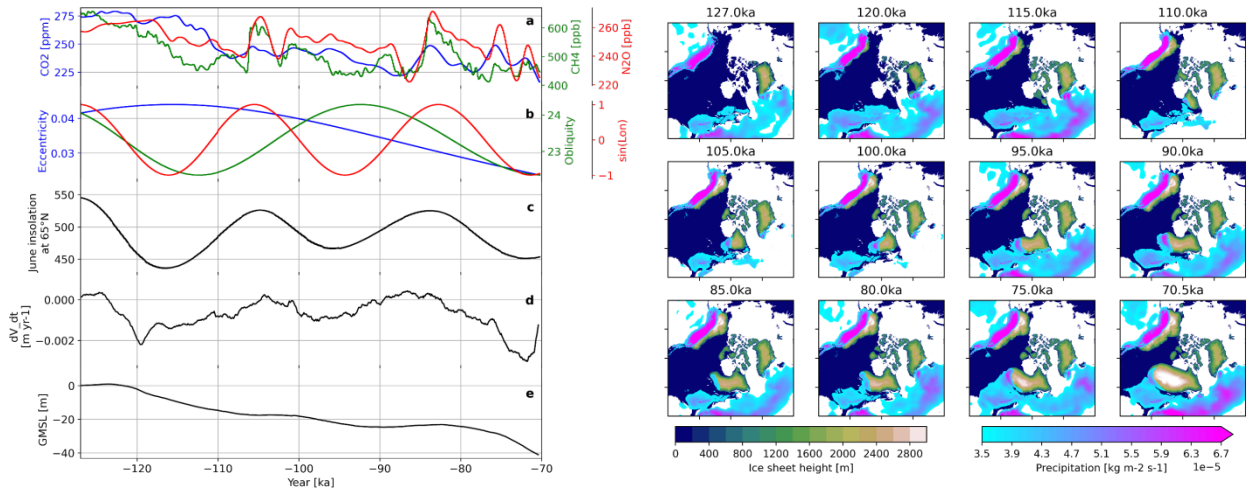

Figure 1: left: *Atmospheric greenhouse gases (a), orbital parameters (b) and summer insolation at 65°N (c) as drivers of the sea level change rate (d) and evolution of global mean sea level relative to 1850 (e) due to simulated growth of the ice sheet;* ***right:*** *development of north American ice sheet height (green-brown shading) and precipitation (blue-red shading) from 127 to 70 ka BP.*

In WP1.1 multi-millennia scenario simulations following four different (SSP2-4.5, SSP4-6.0, SSP3-7.0, SSP5-8.5) scenarios extended following Meinshausen et al. (2020) progressed to year 4000 CE (Fig. 2). Greenland Ice Sheet (GrIS) response to radiative forcing is strongly nonlinear, raising sea level by less than 0.5 m in the lower emission scenarios, but by 4-5 m in SSP3-7.0 and SSP5-8.5. Highest melt rates occur around 2500 CE at highest global average temperature and reduce thereafter even under highest emissions. The GrIS is generally stable both in the south and the mountainous east. Melting is strongest in the west and towards the GrIS center and discharges to Baffin Bay and Arctic Ocean. Linked to increased stratification due to higher heat fluxes in the North Atlantic caused by the warming atmosphere we generally observe reduction in Atlantic meridional overturning circulation (AMOC), by -30% to -60% in SSP2-4.5 and SSP5-8.5. We show that simulated GrIS dynamics, in particular heterogeneity of GrIS discharge, are key to the impact on North Atlantic deep-water formation. We highlight the impact of feedbacks between ice sheet and climate in Earth system models and underline that thermal inertia of ice sheets necessitates integration of models beyond the end of this century.

WP1.2 published research that highlights control of internal climate feedbacks, in particular those related to ice sheet interactions with other components of the complex Earth and climate system, in the evolution of the Eurasian Ice Sheets (EIS) from MIS3 to the LGM. EIS evolution shows bifurcation, where high latitude summer insolation decrease only supports snow and ice cover for subsequent ice volume growth if AMOC is relatively weak, and surface mass balance is nonlinearly linked to precipitation and temperature variations.

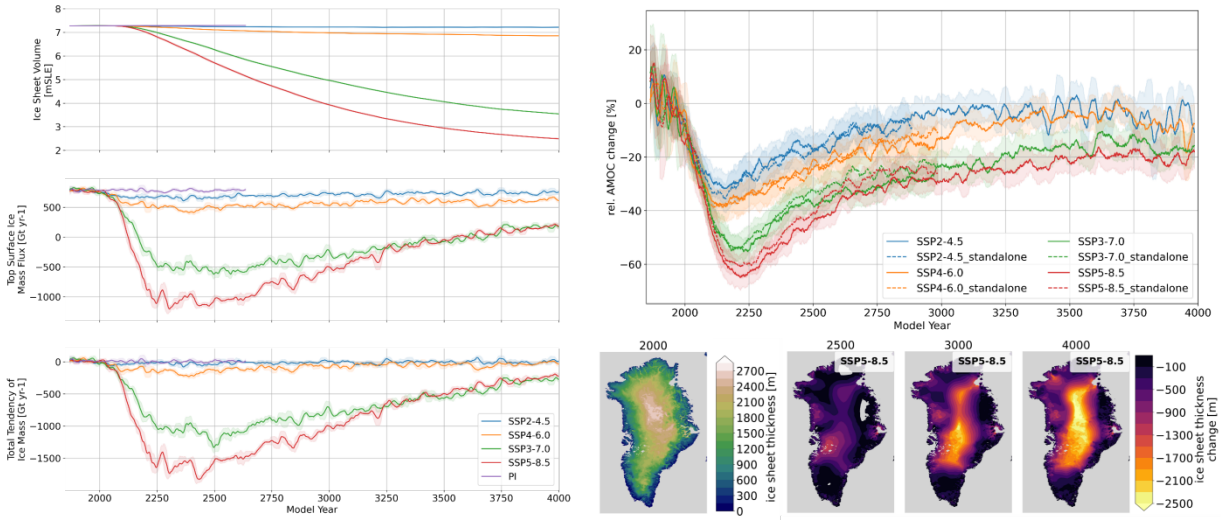

***Figure 2: left**: Simulated GrIS volume and change over time and quantification of surface mass balance in relation to total mass balance; **top right:** AMOC index at 26°N with (solid lines) and without (dashed lines) interactive GrIS; **bottom right:** comparison of simulated future GrIS thickness to year 2000 conditions for the high emission scenario only.*

In WP3.2 we improved representation of glacial climate conditions in AWI-ESM-WISO simulations towards maintaining the vertical temperature and salinity structure in the LGM, resolving the problem of an overly deep and strong upper AMOC branch. To this end, we adjusted two key atmospheric parameters—the relative humidity threshold for cloud formation in the lowest model level and the threshold for separation of cloud liquid water and cloud ice. The LGM shows colder ocean surface, enhanced Southern Ocean sea-ice formation, and a more stable vertical stratification of the Atlantic Ocean (Fig. 3, left).

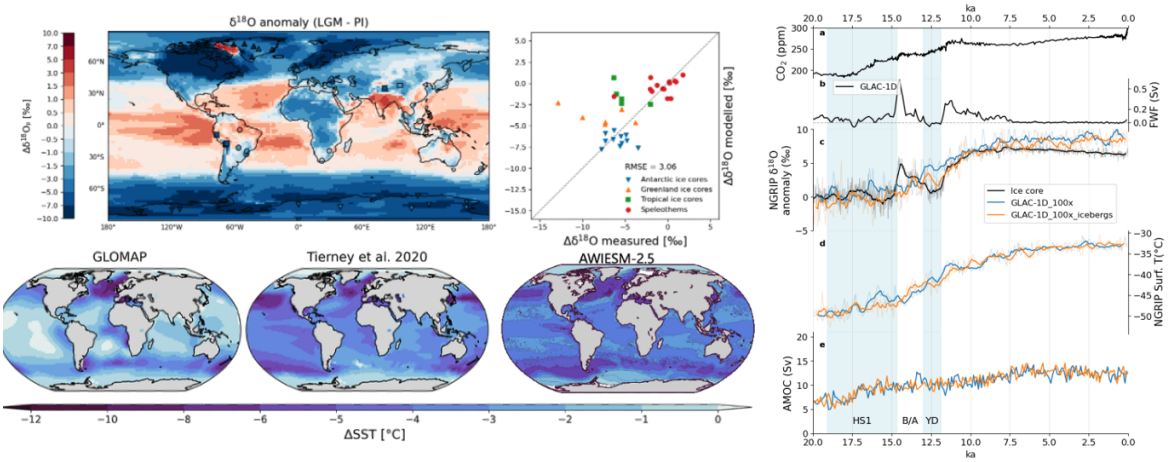

***Figure 3: left:** simulated precipitation δ¹⁸O anomaly (LGM − PI) (top) showing spatial distribution (left) and agreement between simulation and proxies (right); spatial distribution of simulated and reconstructed sea surface temperature (SST) anomaly (bottom); **right:** last deglaciation evolution of observations (black) and simulations with (orange) and without (blue) icebergs; (a) atmospheric CO_2; (b) meltwater flux derived from the GLAC-1D ice-sheet reconstruction; (c) δ¹⁸O, observations from the NGRIP ice core; (d) simulated NGRIP temperature; (e) strength of the AMOC.*

The iceberg module supports realism of freshwater forcing during ice-sheet retreat. By combining near-coastal meltwater discharge with iceberg-derived freshwater fluxes we completed 100 times accelerated transient simulation covering the entire last deglaciation (Fig. 3, right). Setup for the full transient simulations is now finalized, and the model is thereby now ready for production runs in the coming year (see proposal document).

Work at MPI

We continued future simulations with the fully synchronously coupled MPI-ESM-CR-mPISM-VILMA model system (Mikolajewicz et al., 2025) under six different socio-economic pathways (SSPs) prescribing greenhouse gas (ghg) concentrations derived from emission driven Climber-X projections. To capture slow response of ice sheets to ghg forcing and associated temperature increase that is dominated by the SSP, simulations were run until 8000 CE (Fig. 4). Temperature response is dominated by the underlying SSP. Maximum warming ranges between 1.8 K in SSP1-1.9 to 12.6 K in SSP5-8.5, relative to the pre-industrial period (PI). We find a strong temperature response of the ice sheets. The GrIS, the East Antarctic ice sheet (EAIS) and the West Antarctic ice sheet (WAIS) show different sensitivities to the temperature increase of the individual SSPs (Fig. 4). The EAIS exhibits continued ice loss only under the three highest SSPs. GrIS and WAIS show considerable mass loss already for intermediate to low SSPs, respectively. Differences in response relate to different ice sheet characteristics and mass loss dominating processes currently analyzed in more depth. We plan to compare a set of these future simulations to future projections conducted with other coupled ESM-ice sheet models (Climber-X, AWI-ESM and CESM), which requires keeping a substantial amount of model output on /work until the next allocation period.

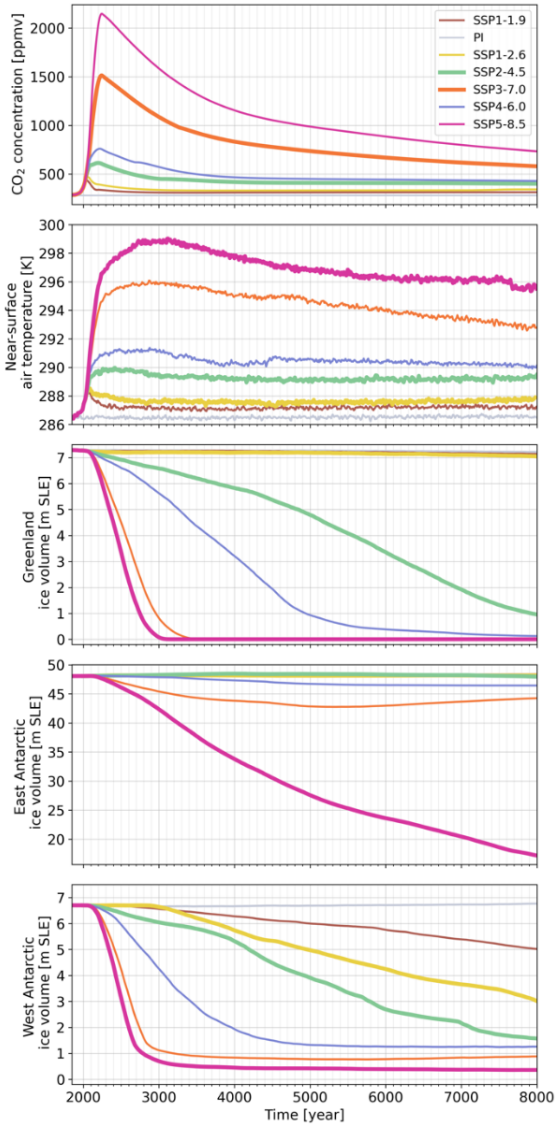

Figure 4: *Future simulations of the climate-ice sheet system under different SSPs, showing CO2 concentration, global near-surface air temperature as well as the ice volume change of the GrIS, EAIS and the WAIS.*

We further applied the model setup, but with an asynchronous coupling, to investigate stability of the GrIS (Andernach et al., 2025). In a comprehensive set of steady state simulations, we find

that at least four steady states exist under PI climate forcing: Besides a state with a large GrIS (L_G) that is similar to the PI state, we find steady states with GrIS volumes of about 48% (M_G), 28% (S_G) and 19% (XS_G) of the PI volume (Fig. 5). These states are stabilized through several feedback processes, such as melt-elevation and melt-albedo feedback. In smaller states, ice sheet expansion is further limited by redistribution of precipitation, Föhn effect, and additional warming driven by atmospheric circulation changes due to the reduced blocking by a smaller GrIS. Southern GrIS is controlled by alterations of the sea-surface temperature of Irminger Sea and Nordic Seas. Additional sensitivity experiments show that interactions between GrIS and Antarctic Ice Sheet (AIS) impact transient behavior of the GrIS. Further threshold experiments indicate that if the GrIS volume drops below a critical threshold of 83-70% of its PI volume, at least half of its current volume will be irreversibly lost even under return to global PI temperatures through a reduction in CO_2 concentrations.

Our study is the first to demonstrate multi-stability of the GrIS in an ESM coupled to an ice-sheet model and to comprehensively investigate how feedbacks with the climate system constrain the steady states. The analysis highlights the importance of a two-way coupling between individual climate components, specifically interactions between ice sheets and ocean, atmosphere and land. Additionally, this work provides evidence that inclusion of dynamic ice sheets in both hemispheres is essential in studies of the stability of the GrIS and AIS due to interactions and teleconnections between them.

Besides future and steady-state simulations, we also continued our efforts on transient simulations of Marine Isotope Stage 3 and last deglaciation with our model system. We started transient synchronous simulations from 49 ka BP to present. This work allows us to assess drivers and processes behind climate variability in the past and their global impacts. Here, we are currently specifically interested in the drivers and impacts of abrupt ice-sheet surges in both Hemispheres.

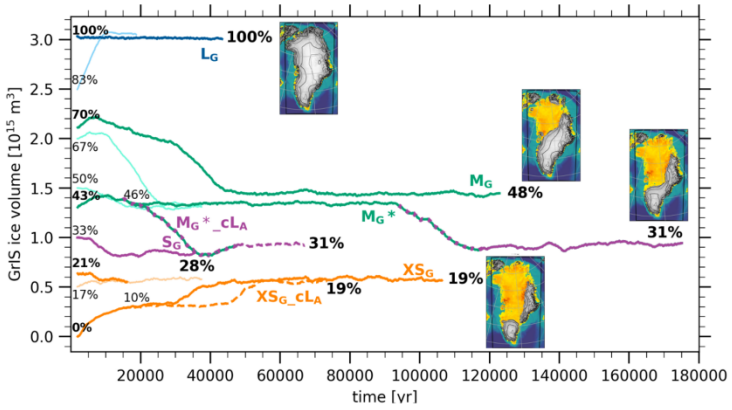

Figure 5: *Multiple steady states of the GrIS. Steady-state simulations performed with interactive ice sheets (Solid lines). Same experiments performed with a prescribed PI AIS from state LG (dashed lines). Threshold experiments constrain the range of initial volumes that are attracted by each steady state of the GrIS (thin, light-colored lines). Initial volumes displayed in small font numbers, initial and final volumes in bold font numbers. Final states also shown as maps of ice thickness in meters of the final steady state GrIS volumes overlaid on the surface bedrock in meters above sea level (m a.s.l.). Percentages relative to the size of the PI iGrIS.*

Work at PIK and GFZ

In TP1 (GFZ) we continued improving and verifying global 3D mantle viscosity structure as input for VILMA by adopting previous viscosity structures based on a priori constraints. We applied the Haskell constraint with the sensitivity kernel given by Steinberger & Calderwood (2006) and updated our suite of 3D viscosity structures described in Bagge et al. (2020). Resulting lithospheric thickness of the ensemble is shown in Fig. 6 (left). Furthermore, we are updating the basis viscosity model obtained through conversion of an updated seismic tomography model to a mantle viscosity structure.

Using these new Earth structures we performed VILMA-3D test runs on Levante. In addition, we continued improving the rotational feedback implementation in VILMA-3D (Klemann et al. in prep) and performed ensemble model runs for VILMA-1D and VILMA-3D with and without the new rotational feedback component in VILMA (Fig. 6).

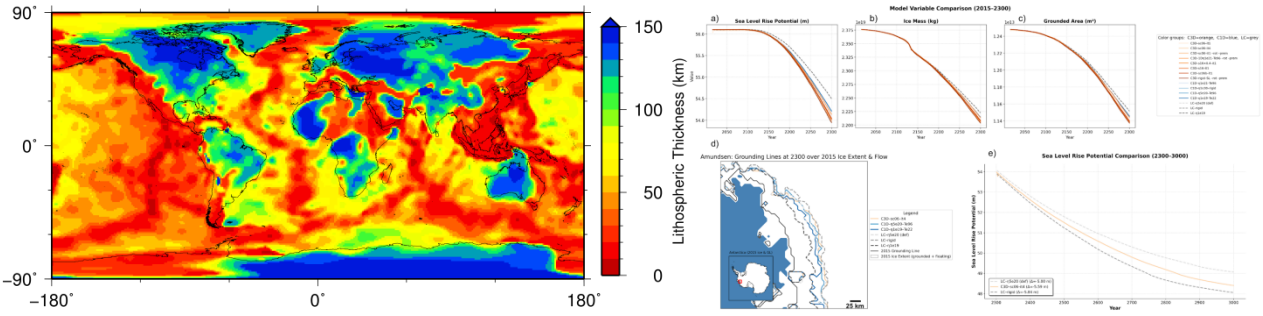

Figure 6: left: Lithospheric thickness (ensemble mean) of updated 3D viscosity structures. The lithospheric thickness is defined by a viscosity threshold of 10^{23} Pas; right: comparison of (a) sea level rise potential, (b) ice mass, and (c) grounded ice area from 2015 to 2300 for different Earth structure models in simulations forced with CESM2-WACCM under SSP5-8.5 using RACMO-derived surface mass balance; (d) grounding line positions in the Amundsen region at 2300; (e) sea level rise potential from 2300 to 3000 for rigid, default LC, and PISM-VILMA 3D Earth structure models.

In TP2 (PIK) of WP1.4 (“Ice sheet instabilities”), we performed PISM-VILMA simulations on centennial time scales with higher resolution than in the glacial cycles simulations by Albrecht et al., (2024). The experimental setup for the entire dynamic AIS is based on the ISMIP6 extensions experiments (Seroussi et al., 2024), where effectively no feedbacks with the solid Earth or sea-level have been considered before. We rerun simulations from 1850 to 2300 with different climatic forcings and for a range of Earth structures (1D and 3D) to quantify the delaying effect of the combined gravitation, rotational and deformational (GRD) response in VILMA on sea-level estimates (see prel. Fig. 6). The results will be presented in a study (Mojtabavi, Albrecht, Klemann, in prep.) and will feedback in the protocol process for ISMIP7. The simulations will be extended to the year 3000 and 12000 using the climatic forcing from CLIMBER-X.

References

Albrecht, T., Bagge, M., & Klemann, V. (2024). Feedback mechanisms controlling Antarctic glacial-cycle dynamics simulated with a coupled ice sheet–solid Earth model. The Cryosphere, 18(9), 4233-4255. doi: 10.5194/tc-18-4233-2024

Andernach, M., Kapsch, M.-L. and Mikolajewicz, U.: Impact of Greenland Ice Sheet Disintegration on Atmosphere and Ocean Disentangled, Earth System Dynamics 16, 451–474, https://doi.org/10.5194/esd-16-451-2025, 2025.

Andernach, M., Kapsch, M.-L., and Mikolajewicz, U.: Stabilizing feedbacks allow for multiple states of the Greenland Ice Sheet in a fully coupled Earth System Model, EGUsphere [pre-print], https://doi.org/10.5194/egusphere-2025-4736, 2025.

Bagge, M., Klemann, V., Steinberger, B., Latinović, M., Thomas, M. (2020). 3D Earth structures for glacial-isostatic adjustment models. V. 1.0. GFZ Data Services. doi:10.5880/GFZ.1.3.2020.004

Gowan, E. J., Zhang, X., Khosravi, S., Rovere, A., Stocchi, P., Hughes, A. L., ... & Lohmann, G. (2021). A new global ice sheet reconstruction for the past 80 000 years. *Nature communications*, *12*(1), 1199.

Klemann, V., Bagge, M., Dill. R. Hagedoorn, J. M., Martinec, Z., Dobslaw, H., (in prep). Rotational deformations in the spectral–finite element code VILMA and consequences for GIA corrections applicable to GRACE and GRACE-FO. Geophys. J. Int.

Meinshausen, M., Nicholls, Z. R., Lewis, J., Gidden, M. J., Vogel, E., Freund, M., ... & Wang, R. H. (2020). The shared socio-economic pathway (SSP) greenhouse gas concentrations and their extensions to 2500. *Geoscientific Model Development*, *13*(8), 3571-3605.

Mikolajewicz, U., Kapsch, M.-L., Schannwell, C., Six, K. D., Ziemen, F. A., Bagge, M., Baudouin, J.-P., Erokhina, O., Gayler, V., Klemann, V., Meccia, V. L., Mouchet, A., and Riddick, T.: Deglaciation and abrupt events in a coupled comprehensive atmosphere–ocean–ice-sheet–solid-earth model, Climate of the Past, 21, 719–751, https://doi.org/10.5194/cp-21-719-2025, 2025.

Mojtabavi, S., Albrecht, T. & Klemann, V. (in prep.), „Delayed Antarctic Ice Sheet response to century-scale warming in interaction with the solid Earth and sea-level“

Niu, L., Knorr, G., Krebs-Kanzow, U., Gierz, P., & Lohmann, G. (2024). Rapid Laurentide Ice Sheet growth preceding the Last Glacial Maximum due to summer snowfall. *Nature Geoscience*, *17*(5), 440-449.

Niu, L., Knorr, G., Ackermann, L. et al. Eurasian ice sheet formation promoted by weak AMOC following MIS 3. npj Clim Atmos Sci 8, 85 (2025). https://doi.org/10.1038/s41612-025-00982-5

Pico, T., Creveling, J. R., & Mitrovica, J. X. (2017). Sea-level records from the US mid-Atlantic constrain Laurentide Ice Sheet extent during Marine Isotope Stage 3. *Nature communications*, *8*(1), 15612.

Schannwell, C., Mikolajewicz, U., Kapsch, M.-L. and Ziemen, F.: A mechanism for reconciling the synchronisation of Heinrich events and Dansgaard-Oeschger cycles. NatureCommunication 15, 2961, https://doi.org/10.1038/s41467-024-47141-7, 2024.

Seroussi, H., et al. "Evolution of the Antarctic Ice Sheet over the next three centuries from an ISMIP6 model ensemble." Earth's Future 12.9 (2024): e2024EF004561. https://doi.org/10.1029/2024EF004561

Spratt, R. M., & Lisiecki, L. E. (2016). A Late Pleistocene sea level stack. *Climate of the Past*, *12*(4), 1079-1092.

Steinberger, B. & Calderwood, A.R. (2006). Models of large-scale viscous flow in the Earth’s mantle with constraints from mineral physics and surface observations. Geophys. J. Int., 167, 1461–1481. doi:10.1111/j.1365-246X.2006.03131.x

Project: 1030

Project title: PalMod WG2

Project lead: Victor Brovkin, Thomas Kleinen

Report period: 2025-01-01 to 2025-12-31

Overview

WG2 of PalMod aims at understanding and quantifying feedbacks between biogeochemistry and climate during glacial cycles. In Palmod III, two work packages are focusing on the terrestrial and the marine carbon cycle.

WP2.1 "Terrestrial processes"investigates the feedbacks between climate and the terrestrial biosphere and carbon cycle for the entire last glacial cycle, with a major focus on the deglaciation and future climate.
WP2.1 partner in this request is MPI-M.

WP2.2 "Marine processes" aims to improve the understanding of feedbacks between ocean biogeochemistry and climate for the last deglaciation and thereby improve the skills of ESMs in projecting the future ocean carbon sink and the changes in the marine environment.
WP2.2 partners in this request are AWI, CAU Kiel and UHH.

Report

WP2.1 "Terrestrial Processes", MPI-M

WP2.1 performs work in three areas: 1) Transient modelling of the coupled global carbon cycle, 2) analysis of land cover changes in model and reconstructions, and 3) the role of remobilised permafrost carbon during the deglaciation.

For modelling the coupled carbon cycle, we completed two full glacial-cycle experiments with interactive methane fluxes but no ocean biogeochemistry, aiming at an evaluation of the long-term changes of vegetation and carbon stocks on land, to explain the rapid changes in GHGs reported in proxy data from polar ice cores. In this long run, climate and vegetation respond to warming (wetting) and cooling (drying) stages of the last glacial cycle, as can be seen in a sequence of biome shifts, which include Saharan greening and boreal tundra expansion (Fig. 1a), which also redistribute the soil carbon stocks. We are interested in detecting when the fastest changes in methane levels occur (Fig. 1b), which could provide insight about land-bound mechanisms for abrupt events. Until now, the fastest and most significant abrupt changes appear in connection with strong AMOC perturbations and tropical vegetation decline.

Considering a fully interactive carbon cycle, we also carried out experiments with dynamic marine biogeochemistry. The added complexity of having transient marine processes increases the computational burden and greatly limits the time range of the experiments. Moreover, many questions remain open about how to simulate a transient deglaciation with a comprehensive climate-carbon system that is able to reproduce the increase in atmospheric CO2 of about 100 ppm since the Last Glacial Maximum (LGM). In our experiments, we choose to implement a nudging function for sea-surface alkalinity to have CO2-concentration change similarly as in geological records. Our results averaged over Antarctica show the expected 100 ppm increase in

CO2, as well as the roughly, 400 ppb increase in CH4(Fig. 1c). Again, the fastest changes in greenhouse gases (GHGs) appear related to strong AMOC disturbances. Although fast in comparison to other parts of the simulation, the changes are not nearly as abrupt as reported from ice-core data.

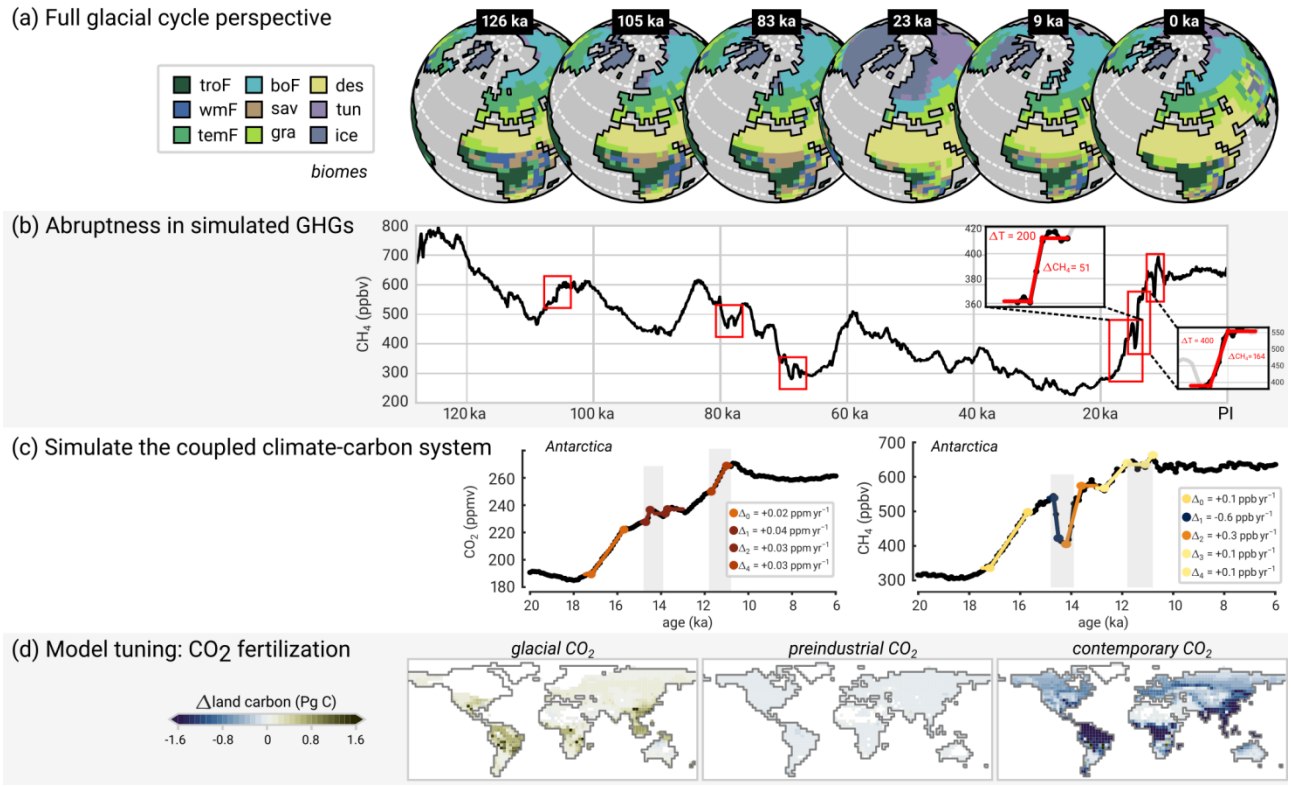

***Figure1**: (a) global vegetation changes of the last glacial cycle, shown as biome shifts in North Africa and Eurasia. (b) detection of related rapid changes in simulated CH4variations. (c) simulated GHGs in Antarctica, highlighting fast changes related to AMOC perturbations. (d) experiments of model tuning for a weaker CO2fertilization show a smaller low/high CO2contrast.*

In our previous work, we found that Earth system models simulate an expansion of the Northern Hemisphere Forest biome following the Last Glacial Maximum that precedes pollen-based reconstructions by several millennia (Dallmeyer et al., 2022). The underlying causes and potential consequences of this temporal discrepancy remained unclear. To evaluate the consequences of a likely too fast forest expansion in the model on future vegetation dynamics and climate projections, we planned to conduct transient simulations for the future under various CO_2 scenarios, both with and without slowed vegetation expansion. To carry out these simulations, the following steps were necessary:

1.) An evaluation of the simulated tree cover against new quantitative vegetation reconstructions, in order to better understand where and why the model produces a too fast forest expansion, also with respect to the simulate tree cover and not only with respect to the assigned forest biome.

2.) To perform test simulations to determine the most effective way to slow down tree cover expansion in the model.

It turns out, that the model-data mismatch arises from two overlapping signals: an underestimation of forest in the boreal latitudes, and an overestimation of forest expansion in the temperate zones. Therefore, it is not appropriate to simply slow down vegetation dynamics as a whole. Instead, forest expansion in boreal latitudes needs to be strengthened, while forest expansion in temperate zones should be slowed.

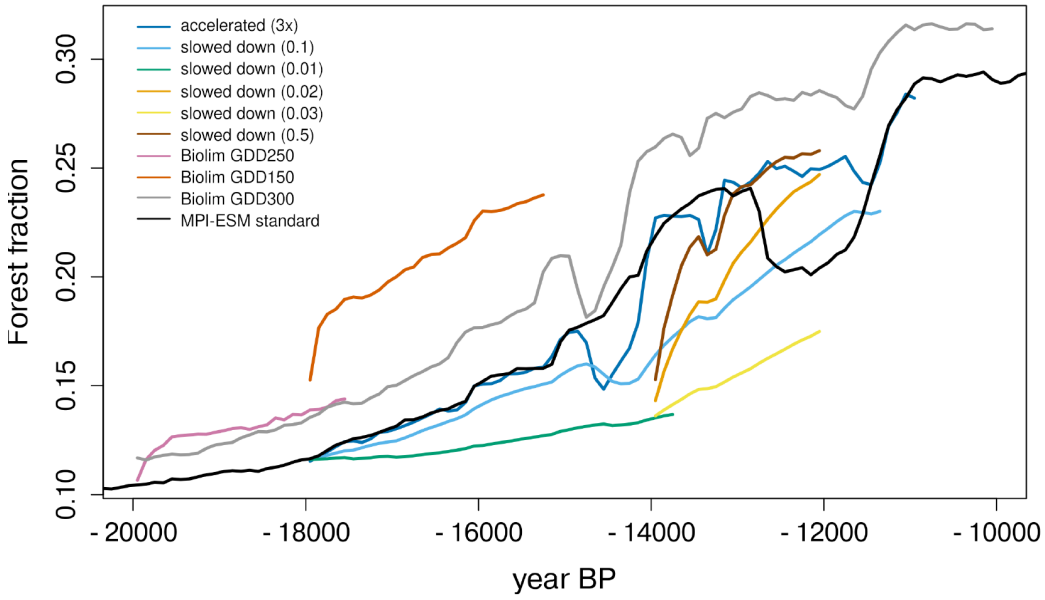

***Figure** 2: Simulated Forest fraction in the NH extratropics in simulations with slowed down vegetation dynamic or enhanced boreal vegetation dynamic (by GDD limit modifications) compared to the standard simulation (black).*

Additionally, we intended to assess the potential climate impacts of simulated forest cover that differs from reconstructions by prescribing land cover aligned with these reconstructions for six key time slices over the past 14,000 years. These simulations turned out to be more challenging than expected, as, for example, in some regions there are not enough reconstructions available or the existing ones are not reliable. Additionally, the Southern Hemisphere was entirely excluded from the reconstructions. As a result, we have not yet found an accurate way to carry out these simulations.

Finally, bringing together a number of recent developments of MPI-ESM, we aim to investigate the role of remobilized permafrost carbon on atmospheric CO2 during the deglaciation; particularly on abrupt rises in CO2 concentrations like that observed at the start of the Bølling-Allerød. During the last year we continued a series of sensitivity tests on the version of the MPI-ESM we aim to use for this study in order to assess and tune the deglacial climate it produced. The optimal parameters for this setup have now been determined that offer a balance between including necessary processes and limiting the impact on the glacial climate in order to avoid needing to fully retune MPI-ESM which would not be feasible just for this study due to limited resources. A deglaciation run has been performed with this setup to study the changing extend of permafrost using this new scheme during this period. A experiment is now ongoing to study the carbon released during the Bølling-Allerød by running a 3000 year transient run centered on this event (in our model) with a spun-up carbon state and deep carbon pools estimated from data.

A more sophisticated evaporation scheme has been now added to our dynamic lake model for modelling lake changes during the last glacial cycle; we have tested this with a partial transient glaciation run covering the most interesting period of the deglaciation for lakes. This proved technically challenging and it was not possible to run the proposed study of differing drainage scenarios in the last year.

WP 2.2 "Marine processes ", CAU Kiel

In 2025, we have so far re-done several MPI-ESM PI time-slice simulations as well as LGM sensitivity experiments with modified mixing, sea-ice and ECHAM parameters using about 5200 node hours (of the approx. 18000 node hours that were allocated to our subproject). The reason for this *originally not planned* repetition was that the North Pacific deep water in the previous simulations was much too old: the simulated age since the last contact with the sea surface was as old as 3000 years at 1500m (Fig. 3b), while estimates using ^{14}C data indicate that the water at 1500m and below has a circulation age of just over 1000 years (see Fig. 4 in Matsumoto 2007). This new setup (which we call *D21mix* here, because it is based on the recently published experiment D2.1 by Mikolajewicz et al. 2025), reduces the age bias significantly due to higher background mixing in the deep ocean compared to our previous setup (called "wkmix", see Fig. 3a). And, at the same time, unlike the previously also used "stmix"-setup, it still leads to a (compared to PI) shallower and weaker meridional overturning circulation in the Atlantic for LGM boundary conditions (Fig. 3c), which is 1) in line with reconstructions and 2) crucial to realistically simulate the deglacial deep ocean carbon reservoir changes. A manuscript describing these time slice simulations is in preparation.

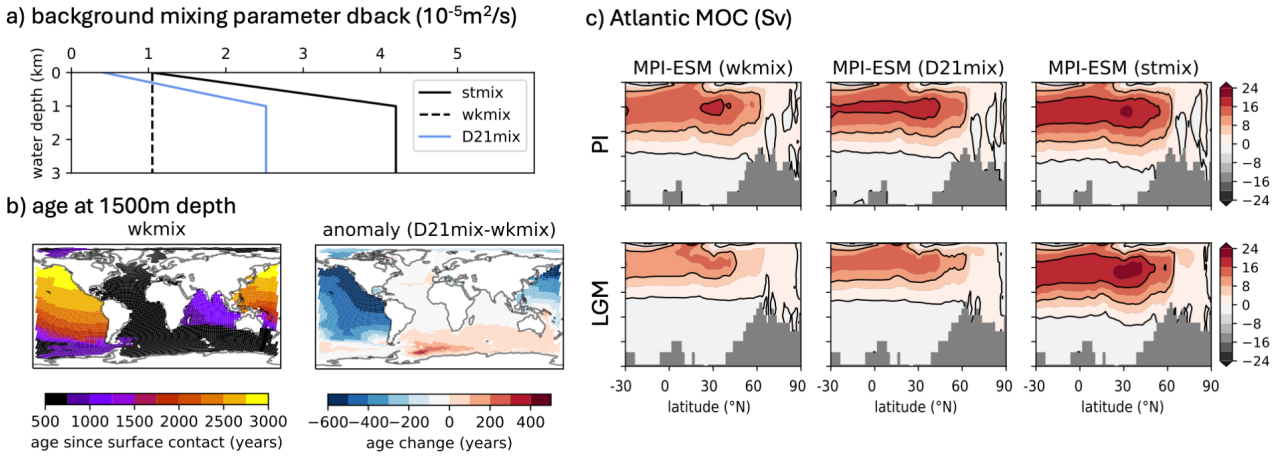

***Figure 3**: Comparison of the different model setups named "wkmix" for weak mixing, "stmix" for strong mixing, and "D21mix" for the new setup with somewhat intermediate prescribed background mixing parameter dback (a); (b) resulting sea water age since surface contact for the "wkmix" experiment and the D21mix-wkmix sea water age anomaly in years; (c) resulting (200-year mean) pre-industrial (PI, top) and Last Glacial Maximum (21ka BP, bottom) Atlantic meridional overturning circulation (MOC).*

The transient deglaciation simulations that we had planned to start or to continue in the beginning of 2025 were consequently postponed. We are planning to re-start our first deglaciation run (which

had gotten stuck after several crashes as reported earlier, and which was based on the "wkmix" setup) in the next weeks using the new D21mix setup to use up our remaining resources.

WP 2.2 “Marine processes “, UHH

By the time of the report (end September 2025), we had utilised 28,225 node hours, exceeding 24% of the allocated node hours for our subproject during the period from January to September (which accounts for 12.8% of the computing time allocated to bm1030). We have conducted simulations with MPI-ESM as previously planned. However, due to the significant reduction in computing time, some planned deglaciation simulations (from 21,000 years ago to the present day) could not be carried out in 2025. Notably, the reduced workspace has become a substantial limitation for our research on ocean biogeochemistry, as many variables require monthly 3-dimensional output, which is essential for comparison with proxy data that often exhibit seasonal biases. Nonetheless, our existing simulations enabled us to address several exciting scientific questions.

A) As the deglacial ocean circulation is subject to significant uncertainties, we investigate its impact on deglacial ocean CO2 outgassing in physical climate models achieved by tuning ocean background vertical diffusivity (hereafter referred to as “Strong-mix” and “Weak-mix” physical models). The Weak-mix model captures the magnitude of the atmospheric CO2 rise during early deglaciation observed in the ice core data. This mainly results from a higher rain ratio and ventilation of high DIC, low alkalinity water masses. We also further conducted model-data comparison for the deglacial global ocean oxygen content. These results have been presented at EGU25 (Liu et al.; Rückert et al.) and the PAGES Open Science Meeting 2025 (Liu et al.).

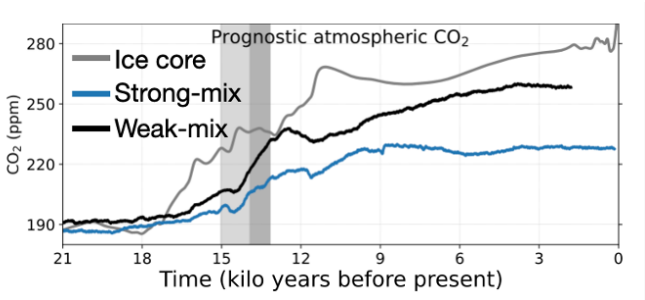

Figure 4*: Atmospheric CO2 evolution during the last deglaciation in MPI-ESM (Strong-mix physical model in blue, Weak-mix physical model in black) and from ice core record (gray).*

B) Using the transient Holocene simulations with additional monthly 3-dimensional oxygen and nutrients data, we find that fluctuations in AMOC exerted a fundamental control on Arabian Sea oxygenation. Intervals of substantially weakened AMOC during deglaciation coincided with transient OMZ retreats, despite generally sluggish ventilation of intermediate- and deep waters, and seasonally ventilated shallow and intermediate waters. A manuscript (Ni et al.) is under preparation with this model-data comparison study.

C) We conducted further sensitivity experiments within the PalMod ocean biogeochemical model intercomparison project (PalMod OBGC-MIP), including the sensitivity of the glacial ocean carbon cycle to dust deposition, and a new set of experiments with the Weak-mix physical model mentioned in A). A manuscript on OBGC-MIP is currently being prepared.

D) We have tuned the M4AGO particle sinking scheme, impacting the marine biological carbon pump (Maerz et al., 2020; Liu et al., 2024), considering the new ecosystem model tuning (which has been applied in deglacial simulations in A). This new tuning will be applied to the glacial simulations (spin-up) and transient deglacial simulations to investigate the impact of organic matter sinking to deglacial ocean CO2 outgassing.

WP2.2 "Marine processes ", AWI Bremerhaven

From January to September 2025, we completed 4 time slice simulations and 2 transient simulations with totally 32700 node hours, about 34% of the computing time requested. During the last three months of the year, we plan to finish 2 time slice simulations with the new version of AWI-ESM (-2.6), some tuning experiments and start three long transient simulations of 2500 years each. With these new simulations we would need about 96000 node hours. Only 51873 node hours, however, are available in the BM1030 account for the entire WP2.

Experiments conducted were:

1. Two short time slice simulations with tuned cloud parameters and bug fixes

One time slice simulations under LGM climate conditions were run for 300 years with different cloud parameters compared to previous LGM simulations.

Another one time slice LGM simulation was run for 300 years with corrected salt flux due to sea ice formation.

These results will be used in the the model inter-comparison projects within WP2.

2. Two time slice simulations with additional preformed tracer for silicate

One PI and one LGM simulation with one additional preformed tracer for silicate were run for 1000 years each.

3. Transient hosing experiments

Two hosing experiments were continued for further 1000 years in total based on experiments started 2024. Different freshwater flux and duration were applied. With these results we were able to show that the higher dust deposition during the LGM indeed led to a decrease in the Si:N ratio in Southern-Ocean-sourced water masses, but that this signal does not reach the surface equatorial region during the LGM, because of the stronger ocean stratification. Instead, there is an increased Si supply after addition of freshwater to the North Atlantic during deglaciation, which leads to a pulsed increase of diatom productivity then (Fig. 2.2-3). The results were presented at EGU 2025 (Ye et al., 2025) and used to prepare a manuscript on the deglacial Si cycle (Ye et al., in review).

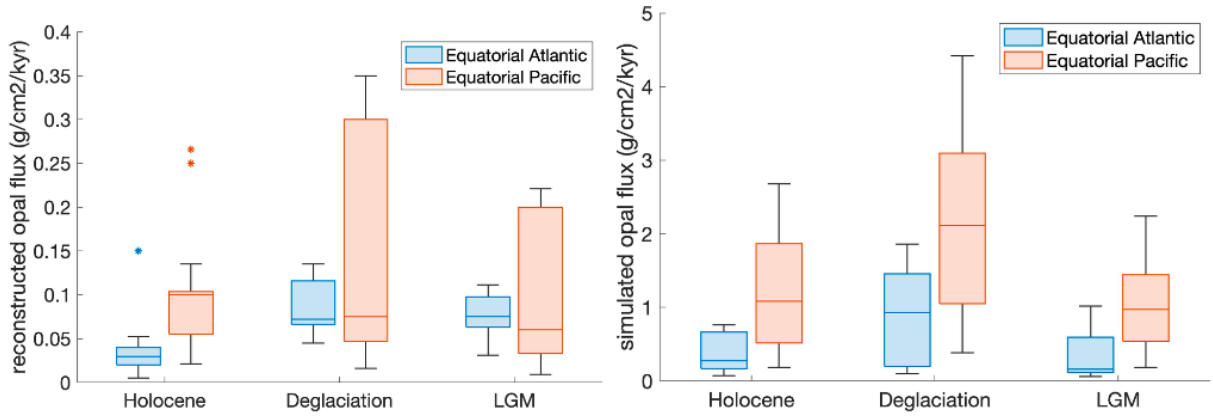

***Figure 5**: Reconstructed ^{230}Th-normalised opal flux (left) in the equatorial Atlantic and the equatorial Pacific for the Holocene (<11 kyr ago), the LGM (19–23 kyr ago), and deglaciation (14.6–18 kyr ago), compared with simulated opal deposition flux at seafloor (right) at the location of reconstructions in the PI simulation, hosing experiment and LG< simulation, all in g opal cm^{-2} kyr^{-1}.*

References

Duque-Villegas, M., Claussen, M., Kleinen, T., Bader, J., and Reick, C. H.: Pattern scaling of simulated vegetation change in North Africa during glacial cycles, Clim. Past Discuss. [preprint], https://doi.org/10.5194/cp-2024-61, in review, 2024.

Ye, Y., Köhler, P., Butzin, M., and Völker, C.: Silicic acid leakage during Last Glacial Maximum and glacial termination, EGU General Assembly 2025, Vienna, Austria, 27 Apr–2 May 2025, EGU25-12616, https://doi.org/10.5194/egusphere-egu25-12616, 2025.

Ye, Y., Köhler, P., Butzin, M., and Völker, C.: Silicon redistribution after Heinrich Stadials stimulated low-latitude diatom growth, in review.

Liu, B., Ilyina, T., Brovkin, V., Willeit, M., Ye, Y., Völker, C., Köhler, P., Heinemann, M., Kurahashi-Nakamura, T., Paul, A., Schulz, M., Merkel, U., and Lhardy, F.: Constraining glacial ocean carbon cycle – A multi-model study, in preparation.

Ni, S., Liu, B., Glock, N., Burdanowitz, N., Lu, Z., Fietzke, J., Ilyina, T., Schmiedl, G., AMOC-driven shifts in Arabian 1 Sea oxygen and nitrogen storage during the last deglaciation, in preparation.

Liu, B., Rückert, E., and Ilyina, T.: Different time scales in the transient response of the ocean carbon and oxygen cycles to deglacial climate change. Oral presentation, EGU25 April 27-May02, Vienna.

Rückert, E., Liu, B., and Ilyina, T.: Impact of past AMOC disruptions on ocean oxygenation. Poster presentation, EGU25 April 27-May02, Vienna.

Liu, B. and Ilyina, T.: Quantifying the impact of AMOC variations on atmospheric CO2 and ocean deoxygenation in the past climate. Oral presentation, PAGES Open Science Meeting, May 21-24, Shanghai, China.

Dallmeyer, A., Kleinen, T., Claussen, M. et al.: The deglacial forest conundrum, Nat Commun 13, 6035, https://doi.org/10.1038/s41467-022-33646-6,2022.

Ye, Y., Köhler, P., Butzin, M., and Völker, C.: Silicic acid leakage during Last Glacial Maximum and glacial termination, EGU General Assembly 2025, Vienna, Austria, 27 Apr–2 May 2025, EGU25-12616, https://doi.org/10.5194/egusphere-egu25-12616, 2025.

Ye, Y., Köhler, P., Butzin, M., and Völker, C.: Silicon redistribution after Heinrich Stadials stimulated low-latitude diatom growth, in review.

Maerz, J., Six, K. D., Stemmler, I., Ahmerkamp, S., & Ilyina, T. (2020). Microstructure and composition of marine aggregates as co-determinants for vertical particulate organic carbon transfer in the global ocean. Biogeosciences, 17(7), 1765–1803. https://doi.org/10.5194/bg-17-1765-2020.

Liu, B., Maerz, J., and Ilyina, T., 2024. Glacial Atlantic carbon storage enhanced by a shallow AMOC and marine aggregates sinking. Geophysical Research Letters, 51, e2024GL109736, doi.org/10.1029/2024GL109736.

Project 1192

Project title: PalMod Data Project

Project lead: Swati Gehlot (DKRZ)

Report period: 2025-01-01 to 2025-12-31

Overview

The project is led by PalMod phase-III cross cutting working group Data Hub (subproject CC1) which manages the model data produced. The project is used by WG1, WG2, WG3.

The project was created as a data project as an integral part of the PalMod Phase II Verbundprojekt CC.2 in 2021.

Project bk1192 continues the work from Phase II and provides the “PalMod internal data pool” that stores and manages core results and data within the phase-II and phase-III scientific modelling WGs. This allows researchers from other work packages and working groups to use these data sets of common interest. Besides facilitating the intra-project collaboration, we assume that this will maximize data reuse while minimizing duplication of datasets on multiple accounts.

For this, all PalMod scientists, who need access to that data pool, which will be created during the runtime of the project PalMod and stored under account bk1192, will become members of the project. The project is expected to exist throughout the phase-III project runtime and possibly afterwards provide a space, where the scientific community will still be able to access and work with the (adhoc)data.

Summary of the work in 2025

Workflows detailing the import, access, share and distribute the data via the common data pool supplied by bk1192 are further developed (and distributed PalMod-wide) in close collaboration with the scientists with respect to their concrete requirements in the year 2023-2025. Along with being a core space for internal data sharing within the PalMod scientific WGs, the data pool bk1192 is also a dedicated space for DataHub-CC1 development and extension of model specific CMORization and publication workflows. Figure 1 shows the systematic usage plan of bk1192 for inflow and outflow of PalMod data.

Resources in 2025

The resource request for 2025 has included mainly Lustre work space (250 TB). As the space is used not only for data provision but also for data standardization, the total amount of usage does not reflect the real needs. The demand is significantly higher during the process of standardization. Original data which was needed after the standardization is deleted from work as soon as possible.